Local Speed Functions in Level Set Based Vessel Segmentation

Rashindra Manniesing and Wiro Niessen

Image Sciences Institute
University Medical Center Utrecht
The Netherlands {rashindra,wiro}@isi.uu.nl

Abstract. A new segmentation scheme is proposed for 3D vascular tree delineation in CTA data sets, which has two essential features. First, the segmentation is carried out locally in a small volume of interest (VOI), second, a global topology estimation is made to initialize a new VOI. The use of local VOI allows that parameter settings for the level set speed function can be optimally set depending on the local image content, which is advantageous especially in vascular tree segmentation where contrast may change significantly, especially in the distal part of the vascular. Moreover, a local approach is significantly faster. A comparison study on five CTA data sets showed that our method has the potential to segment larger part of the vessel tree compared to a similar global level set based segmentation, and in substantially less computation time.

1 Introduction

Vessel segmentation in computed tomography angiography (CTA) data sets remains an important image processing task. Usually, segmentation is the first step in quantification, visualization, pre-operative planning, 3D vessel modeling or in the design of computer aided diagnostic systems. Given its importancy, numerous methods have been developed; an attempt in [6] is made to categorize the different methods that have appeared in literature. In this work we consider level set based approaches [9, 13] for vessel segmentation. Level set evolution is a way of describing the movement of surfaces by embedding them as the zero level set of a higher dimensional function, thereby obtaining an intrinsic, *i.e.* parameter free representation, gaining topological flexibility, and allowing for a simple calculation of geometrical properties, such as curvature, of the moving surfaces. These properties make the level set framework a suitable choice for describing the complex structures of vessel trees.

The crucial factor that determines the success of level set segmentation is the speed function that evolves the surface to the desired boundaries. Typically, most of these speed functions are of a *global* nature, *i.e.* , the same speed function is used at all voxel locations in the image and is often completely pre-computed. There are two important reasons for changing from a global to a local perspective, especially in the case of angiography data sets. First, image contrast is often varying owing to different concentrations of contrast agent, vessel resolution, or

C. Barillot, D.R. Haynor, and P. Hellier (Eds.): MICCAI 2004, LNCS 3216, pp. 475–482, 2004.

in case of magnetic resonance imaging, coil inhomogeneities. Second, the vessel voxels only count for a few percentage of all voxels in the data sets and therefore a local approach would be computationally more efficient. In this paper we propose such a local scheme which is based on level set evolution for carrying out the local segmentation.

The idea of a local adaptive segmentation scheme is certainly not new. However, to the best of our knowledge, only very few adaptive local approaches are proposed in literature. This is perhaps due to the fact that local segmentation is often considered as merely a technical, or implementation issue of a (global) segmentation method. Still, the most closely related work we have found, is given by [5, 11, 1]. Generally speaking, these methods do have a variant of a locally adapting function for segmentation (for instance, the adaptive thresholding technique described in Jiang et al. [5] or the speed function based on statistics that is periodically updated during evolution, in Pichon et al. [11]), but differ essentially in the *dependency* that exist of each local segmentation function on the previous functions at every global iteration step, while we assume a complete independent segmentation function (*i.e.* speed function) for each local volume of interest (VOI).

Our contribution is twofold; first, selection of the next local VOI is done in a novel way by simply estimating the topology of the global segmentation result by skeletonization, and marking those skeleton points which have largest distance from the root point as the new seed points for a subsequent local segmentation. Second, we have applied our proposed method to five realistic, CTA data sets of the brain vasculature, and evaluated these local results with the result obtained by evolving a similar, global level set evolution with constant speed function.

2 Method

The proposed method is as follows (see also Figure 1).

0. Initialization. The user is required to place the first seed point at the root of the vessel tree of interest.
1. VOI selection and local speed function determination. A boxed VOI symmetrical around the seed point is determined for carrying out the local segmentation. An intensity histogram from voxels around a rough segmentation of the vasculature is used to construct the local speed function.
2. Local segmentation by level set evolution. The speed function is used to steer a level set which is iterated until convergence.
3. Topology extraction and labeling. Topology extraction is performed by skeletonization of the global segmentation results, followed by a labeling of the skeleton points. The selection of the next seed points is based on the resulting labeling and distances. Of interest are these end points having the largest distances from the seed point.

Steps 1-3 are repeated. The *global* stopping criteria for a locally adaptive scheme becomes crucial now, since we want to prevent the method to adapt to

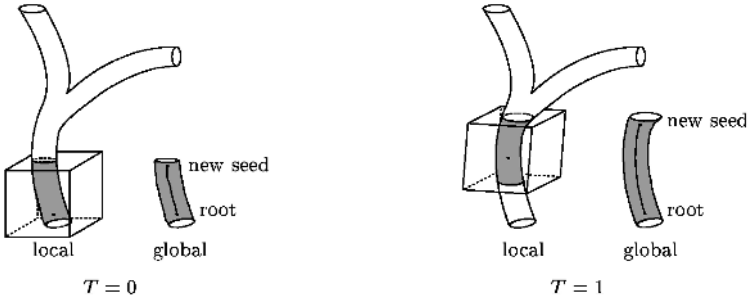

Fig. 1. The local segmentation result adds up to the global segmentation result of which the topology is estimated by skeletonization; the end points from this skeleton are then selected as the next seed points. This way, the orientation of the next volume of interest is implicitly taken into account. Disadvantage is that subsequent local volumes may overlap, for at most half their sizes.

background. Since this a research topic on its own, the discussion is postponed, and we simply set an upper limit on the overall number of local segmentations, as stopping criteria.

2.1 VOI Selection and Local Speed Function Determination

Given a seed point, the VOI is simply chosen symmetrical around this point, and its size should be such, that in this volume the intensity values of vessel and background are approximately homogeneously distributed. This is determined once for a data set by visual inspection. The size can not be too small since then the resulting histogram would not be properly defined. This is important, because the speed function depends on this histogram. The size remains fixed throughout execution of the algorithm. After the VOI has automatically been selected, an initial threshold value is applied to get a rough segmentation of vessel voxels. This initial threshold value is obtained by taking the mean voxel value in a small neighborhood of a few millimeters around the seed point. This neighborhood is set approximately equal to the distance of the seed point to the vessel border. After thresholding, the morphological operations erosion of one voxel width (to remove any noise voxel that may have occurred) and subsequentially dilation of three voxels width (to ensure we include the background, *i.e.* voxels surrounding the vessel voxels, as well), are applied. The resulting histogram is then used to construct the speed function - from now on denoted as the external, image based speed function F_{ext}, as follows[1], see also Figure 2 (the derivation follows the line of a previous paper on this subject [8]).

Two Gaussian distributions g_v and g_b are fitted, using an expectation maximization algorithm [2], and the histogram is then described as (approximately)

[1] Including spatial and higher order information could in principle, improve the results, but for showing the the main ideas of our method, intensity information suffices.

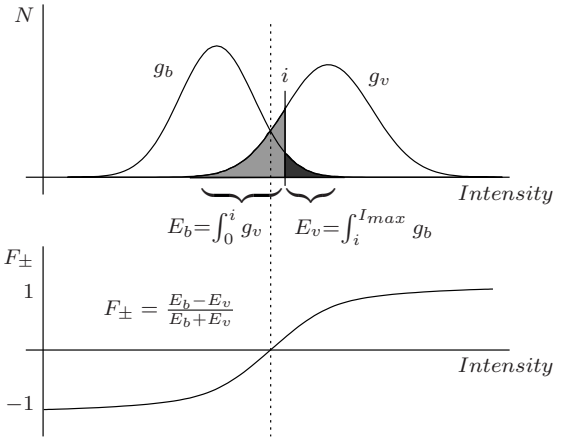

Fig. 2. From histogram to speed functions by classification error functions.

the sum of these functions. The Gaussian distributions overlap and therefore thresholding the image results in misclassifications of voxels; denote E_b and E_v as the fraction of voxels erroneously denoted as background and vessel voxels, *i.e.* $E_b(i) := \int_0^i g_v(x)\,dx$ and $E_v(i) := \int_i^{I_{max}} g_b(x)\,dx$. We propose the following function for F_{ext}

$$F_{ext} := \frac{E_b - E_v}{E_b + E_v} \tag{1}$$

with range $[-1, 1]$ and with $E_b + E_v$ as a normalization factor. F_{ext} is zero at the optimal threshold value (optimal with respect to the total error given by the sum of E_b and E_v), has positive value if the number of misclassified background voxels is larger than the number of misclassified vessel voxels, and vice versa, thus giving rise to positive speed function values inside the vessel, zero at the boundary, and negative values outside the vessel. The negative range of the speed function combined with a smoothness constraint on the evolving level set, is particular effective in preventing possible leaking of the level set evolution through the vessel boundaries when started within the vessel.

2.2 Local Segmentation

Segmentation in the local volume is performed by applying level set evolution [9,13]. The basic partial differential equation is given by $u_t + F|\nabla u| = 0$, with u the signed distance function, u_t the partial derivative to time, and F some general speed function. In image segmentation, F is often defined as $F := F_{ext}(c - \epsilon\kappa)$ (first proposed in [3,7]) , with F_{ext} the image based term (previously defined in Equation 1), $c := 1$ a constant advection term (similar to a balloon force [4]), and $\epsilon\kappa$ a weighted curvature term assuring smoothness of the surface. See [4,12] for more detailed derivations and motivations of the same and related PDEs and related image based speed functions. The curvature on a point on a 3D surface

can be decomposed in two directions perpendicular to each other, in which the curvature takes minimal and maximal value; these extremal curvatures are called the principal curvatures. For vessel structures we prefer a smoothness along the longitudinal direction in which the curvature term is minimal, and therefore we define κ as $\kappa := \kappa_{min}$. Together, they yield our final differential equation

$$u_t + F_{ext}(1 - \epsilon\kappa_{min})|\nabla u| = 0 \tag{2}$$

Evolution is started at the seed point and continued until convergence, *i.e.* stopped if there was no change in segmented volume.

2.3 Topology and Labeling

After convergence of the level set evolution, the zero level set is extracted and combined with the previous segmentation results by the boolean operator OR to get the global segmentation result. OR-ing the results is fast and accurate enough for topology estimation, however, a much cleaner and consistent approach, especially for obtaining the final global segmentation result, would be to merge the borders by applying level set evolutions again, but now initialized by the local results. For now, we choose the first solution. The topology of the global segmentation is then estimated by a 3D skeletonization algorithm [10] based on thinning. Thinning deletes border points of the object satisfying certain criteria until the resulting object does not change any more. The final result of the thinning procedure is a connected, topological preserving skeleton of the original object that is a representation of the central vessel axis part of the vascular tree. In [10] they are called the medial lines, *i.e.* 1D structures in 3D space, making this 3D skeleton algorithm particular suitable for representing the vessel structures.

The resulting medial lines are of only one voxel thick which simplifies labeling. The purpose of labeling is to provide sufficient information to select the next seed points for continuation of the global segmentation. A straight forward algorithm is depicted. First, labeling is started at the root point, which is the seed point or the nearest skeleton point if the seed point is not in the set of skeleton points. The root point is then initialized with distance zero. From the root we traverse the skeleton and for every skeleton point the Euclidean distance is updated and a label is given, either {(E)nd, (S)egment, (B)ranch}, depending on the number of neighbors. That is, if the number of neighbors of a given point minus one equals zero, the point is labeled 'E', equals one, the point is labeled 'S', equals two or more, the point is labeled 'B'. Giving the labeling and distances for each skeleton point, the next seed points are simply those end points having the largest distance from the root point.

3 Experiments and Results

The method is applied to cerebral CTA data sets acquired at the radiology department of the University Medical Center (UMC), Utrecht. A large num-

ber of scans of patients are made on a 16-slice CT scanner (Philips), resulting in data sets of 512×512 by approximately 300 slices, with voxel sizes of 0.3125×0.3125×0.5 mm. Five scans of patients are selected who are examined for screening and showing no signs of hemorrhage (bleeding). Of each patients two scans are made; a low dose scan without contrast, showing bone only, and a high dose scan with contrast, showing bone and vasculature. First bone masking is applied [14]; which consists of rigid registration (based on mutual information and trilinear interpolation), erosion/dilation for noise removal and compensating for inaccuracy of registration, and finally thresholding with T_{bone} and masking. T_{bone} is not critical because the gap between the upper bound of vessel intensity (∼500 Hounsfield Units HU) and the lower bound of bone intensity (∼800 HU) is around 300 HU. Bone masking is not mentioned as part of our method since it is not essential for communicating the main idea of our method. Then, each data set was split into two region of interests - denoted left and right, because the method expects only one seed point for initialization (conveniently chosen at the internal carotid arteries) and which indeed is, of only a technical limitation, and will be removed in a future implementation of our method. The user required input consist of (i) setting T_{bone} (we choose $T_{bone} := 600$ HU), (ii) selection of the initial seed point at the root of the vessel tree, (iii) setting of the global parameters (by lack of an appropriate stopping criteria, the maximum number of local segmentations is set at 25, the size of the local VOI is set at 100×100×100) and finally, (iv) setting of the local, *i.e.* level set parameters. Their values are empirically determined; the number of iterations $n := 1500$ (all local level set evolutions converged before n either by reaching the vessel boundaries, or reaching the bounding box of the VOI in case of adapting to background that sometimes happened during the last VOIs), time step $t := 0.1$, bandwidth $b := 6$, and $\epsilon := 0.35$. Initializiation of the level sets occur in a small sphere of radius two voxels around the seed points. The level set evolution has been implemented using the narrow band method [13].

The evaluation of segmentation methods is important and difficult, and this work forms no exception. A comparison study is conducted and we evaluated the results of our method with the results of a similar global level set evolution, by visual inspection. This global level set evolution starts at the same seed points and has the same parameters as the local level set, except for the number of iterations that now was set at $n := 10000$. To get an impression of the data sets and results, maximum intensity projections of three typical results out of five data sets are shown in Figure 3; the first column gives the original data set (bone masked), the second column the result of the global level set evolution and the third column the results of the locally adaptive segmentations. On average and based on all five results, the local segmentation method captures more vessel structures than the global level set evolution does. In the figure some typical regions of interests are denoted with arrows. For example, the arrow of the first row points at a region the method is erroneously adapting to background. The arrow of the second row points a vessel at which the method discontinues the selection of next VOIs. This is due to seed point selection which only consider

those end points with maximal distance from the root point, thereby running the risk of missing some important end points. The improvement in computation time was significant, about 500 minutes on average for the global segmentation compared to 130 minutes on average for both local segmentations (left and right summed up) of each data set, on the same machine. Clearly, these results are very pleminary, but still gives an indication of the potential of the method.

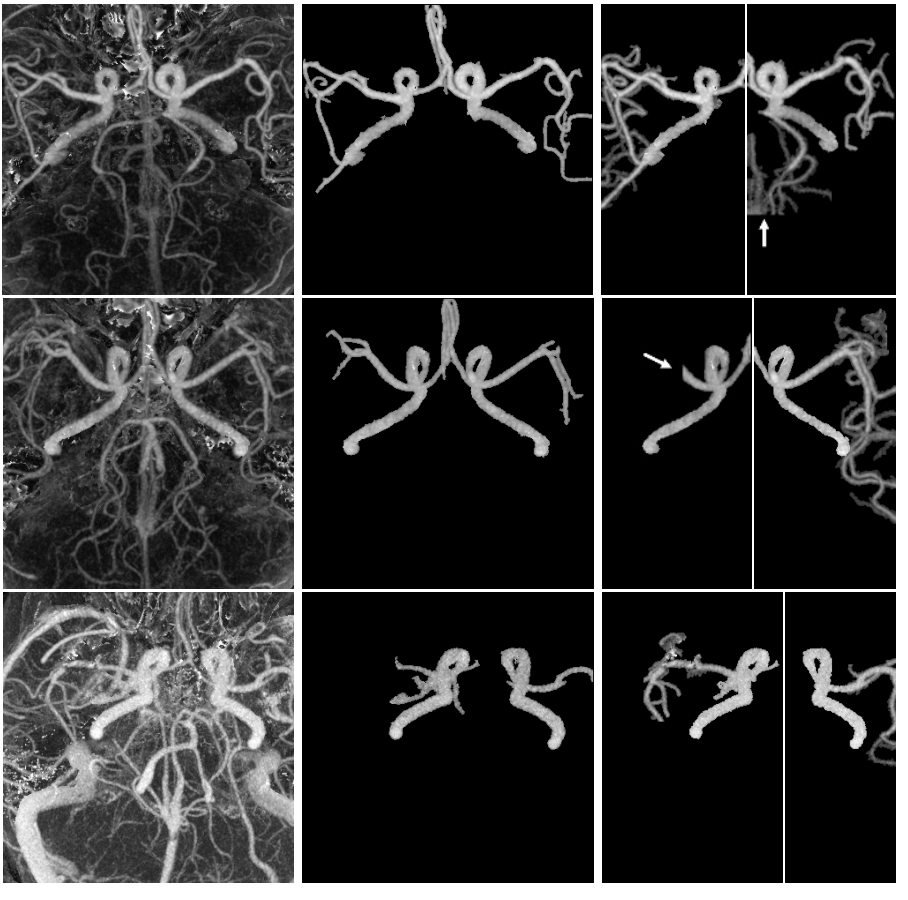

Fig. 3. Three out of five results; first column the original bone masked, second the global result, third the local results. The local results are splitted for technical reasons. Some regions of interest are denoted by arrows, see the main text for an explanation.

4 Conclusions

A new local adaptive segmentation scheme is proposed based on level set evolution for carrying out the local segmentation, and topology estimation by skele-

tonization of the global segmentation for selection of the next volume of interest. A comparison study of our method to a similar global level set evolution on five real, CTA data sets, showed that on average larger parts of the vessel tree are segmented initialized by a single seed point only, and showed a significant decrease in computation time. Future work is to devise a more intelligent, global stopping criteria, to refine the next seed point selection, to include bone masking in the local segmentation, and to conduct a better evaluation study based on a larger patient groups.

References

1. S.R. Aylward and E. Bullit. Initialization, noise, singularities, and scale in height ridge traversal for tubular object centerline extraction. *IEEE Transactions on Medical Imaging*, 21(2):61–75, February 2002.
2. C.M. Bishop. *Neural Networks for Pattern Recognition*. Oxford University Press Inc, New York, 1995.
3. V. Caselles, F. Catte, T.Coll, and F.Dibos. A geometric model for active contours. *Num. Math*, 66:1–31, 1993.
4. V. Caselles, R. Kimmel, and G. Sapiro. Geodesic active contours. *International Journal of Computer Vision*, 22(1):61–79, 1997.
5. X. Jiang and D. Mojon. Adaptive local thresholding by verification-based multithreshold probing with application to vessel detection in retinal images. *IEEE Transactions on Pattern Analysis and Machine Intelligence*, 25(1):131–137, January 2003.
6. C. Kirbas and F.K.H. Quek. Vessel extraction techniques and algorithms: A survey. In *Proceedings of the Third IEEE Symposium on BioInformatics and BioEngineering (BIBE)*, 2003.
7. R. Malladi, J.A. Sethian, and B.C. Vemuri. Evolutionary fronts for topology independent shape modeling and recovery. In *Proceedings of the Third European Conference on Computer Vision*, pages 3–13, 1994.
8. R. Manniesing, B. Velthuis, M. van Leeuwen, and W. Niessen. Skeletonization for re-initialization in level set based vascular tree segmentation. In *SPIE Medical Imaging*. SPIE, SPIE, 2004.
9. S.J. Osher and J.A. Sethian. Fronts propagation with curvature dependent speed: Algorithms based on Hamilton-Jacobi formulations. *Journal of Computational Physics*, 7:12–49, 1988.
10. K. Palágyi and A. Kuba. A 3d 6-subiteration thinning algorithm for extracting medial lines. *Pattern Recognition Letters*, 19:613–627, 1998.
11. E. Pichon, A. Tannenbaum, and R. Kikinis. A statistically based surface evolution method for medical image segmentation: Presentation and validation. In *Medical Image Computing and Computer-Assisted Intervention*, volume 2, pages 711–720, 2003.
12. Guillermo Sapiro. *Geometric Partial Differential Equations and Image Analysis*. Cambridge University Press, 2001.
13. J.A. Sethian. *Level Set Methods and Fast Marching Methods*. Cambridge University Press, second edition, 1999.
14. H.W. Venema, F.J.H. Hulsmans, and G.J. den Heeten. CT angiography of the Circle of Willis and intracranial internal carotid arteries: Maximum intensity projection with matched mask bone elimination - feasibility study. *Radiology*, 218:893–898, 2001.